HEWLETT PACKARD

Control System Loop Gain Measurements

Application Note 243-5

Revised

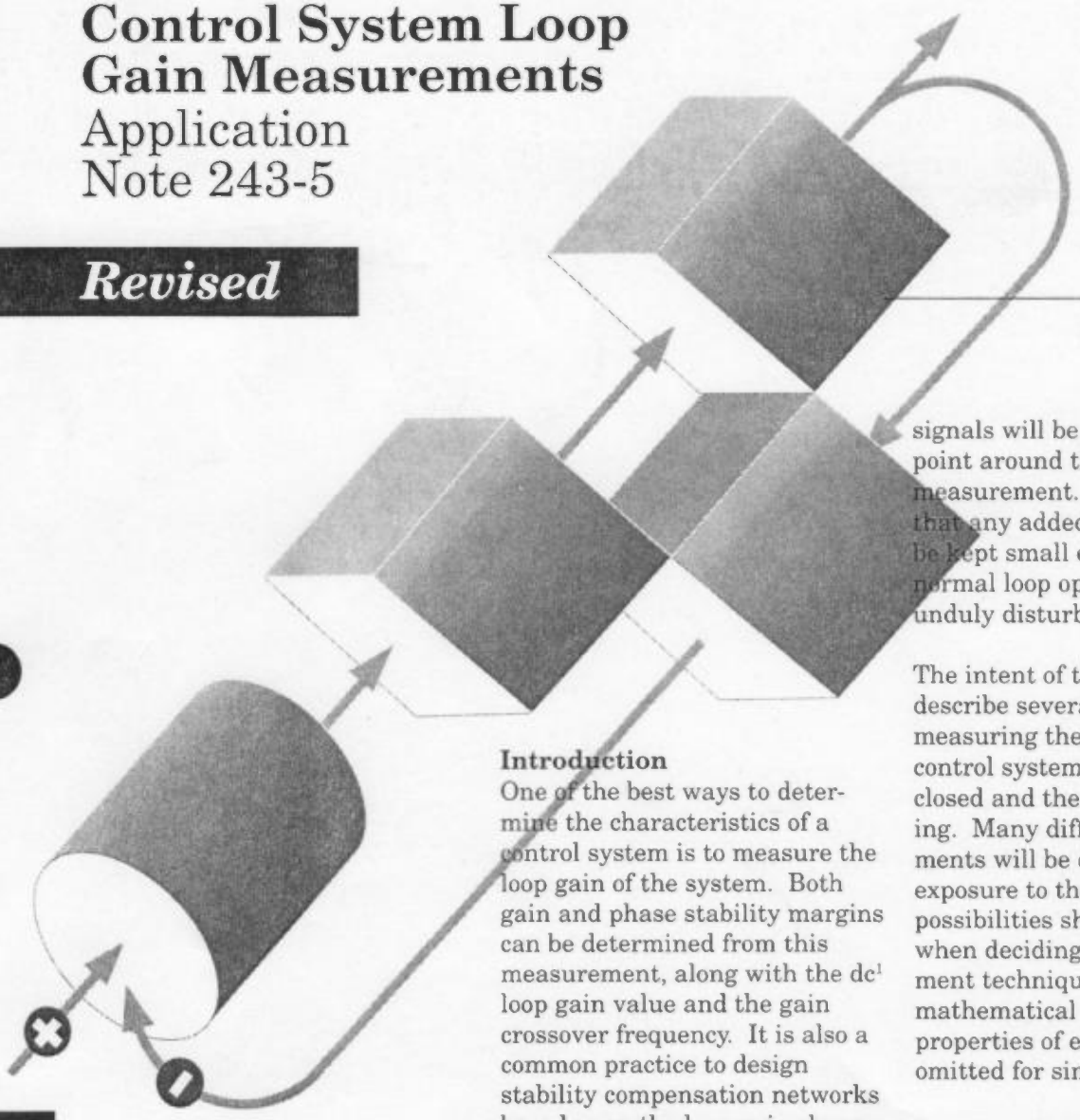

Introduction

One of the best ways to determine the characteristics of a control system is to measure the loop gain of the system. Both gain and phase stability margins can be determined from this measurement, along with the dc[1] loop gain value and the gain crossover frequency. It is also a common practice to design stability compensation networks based upon the loop gain characteristic. Finally, the loop gain of the system is extremely important when defining or refining a model for the control system.

Unfortunately, it is often difficult or impossible to actually open the loop to measure the loop gain directly. Generally, the control system must be operating in a normal manner during the measurement to maintain the proper dc operating point and to minimize distortion. This implies that normal operating signals will be present at each point around the loop during the measurement. It also implies that any added test signal must be kept small enough that the normal loop operation is not unduly disturbed.

The intent of this note is to describe several methods of measuring the loop gain of a control system while the loop is closed and the system is operating. Many different measurements will be discussed. This exposure to the wide variety of possibilities should prove useful when deciding which measurement technique to use. The mathematical derivation of the properties of each method will be omitted for simplicity[2].

It is recognized that nonlinearities and distortion are important in control system testing, but it is beyond the scope of this note to cover these topics. Reference [1] provides some help in these areas.

[1]Direct current. In this note, "dc" will be used to refer to the frequency zero Hertz.

[2]These details are available in reference [3].

W10E

Loop Gain

Loop gain is the term used to descibe the product of the gains of the elements in the control loop that is being investigated. The loop gain of the generic control loop shown in figure 1 is equal to G_1G_2H where the G_i elements are in the forward path and the H element is in the feedback path. Because of this definition, the expression "GH" will be used to indicate "loop gain" throughout the rest of this note.

As a rule, there are at least three regions of interest in the loop gain measurement. Generally, the region of most interest is near unity gain, where both gain and phase margins are measured. Nearly all of the measurement techniques to be discussed work well in this region. As an additional bonus, the ratio of the standard deviation to the expected value of the loop gain measurement (called noise-to-signal ratio in this note) tends to be smallest here.

The next interesting region is often near dc, where the magnitude of the loop gain tends to be large and where a low frequency pole is often located. The actual dc loop gain magnitude determines the steady state error in the output of the control system. Large loop gain magnitudes tend to be difficult to measure. Some methods are much better than others for making measurements in high-gain regions. This will be discussed in more detail later in the note.

The third area of interest is in the high frequency region (near or beyond the gain crossover point) where problems with control system resonances tend to be most severe. Unfortunately, in this region the loop gain magnitude is often small, so the noise-to-signal ratio on the measurement may be relatively large.

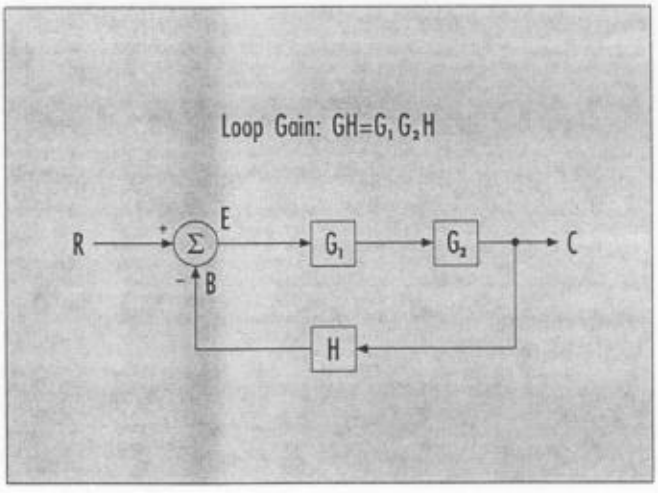

Figure 1 Block diagram of a generic control loop, showing the standard notation for signals and elements.

Measurement Methods

There are many different ways to measure the loop gain. The decision of exactly which one to use in a particular case depends upon several factors. No matter which method is chosen it is necessary to be able to inject a test signal (usually called the excitation signal) into the loop and measure the signal that is present at two (or more) places in the loop. The excitation may be injected into the loop by replacing the normal reference signal, R, or by using a summing junction. If there is not an unused input on an existing summing junction, a new summing junction can be added to the control system. The added summing junction can be either inside the control loop (internal junction) or outside the loop (external junction).

In general, there are two basic "types" of measurements that can be performed: measurements built around the Fast Fourier Transform (FFT) and those built around the Swept Fourier Transform[3] (SFT). These types of measurements are often distinguished by the characteristics of the excitation signal needed. In this note, "broadband excitation" implies measurements based on the FFT, while "swept sine excitation" implies measurements based on the SFT. A brief comparison of these two techniques is included in appendix A.

[3]Measurements built around the Swept Fourier Transform are sometimes called Swept Fourier Analysis or SFA methods.

Three techniques for injecting the test signal from outside the loop ("external" techniques) are shown in figure 2. Two ways to inject the signal inside the loop ("internal" techniques) are shown in figure 3. This note describes measurement methods that are based upon the block diagrams shown in figures 2b and 3a. When using any other injection technique, these equations will have to be revised.

In either case, only certain signal pairs (two of the three terminals of the injection device, for instance) may be available or convenient for use in the measurement. Eight methods are actually needed to cover all possible combinations of signal pairs, and each of these methods can be implemented using either swept sine or broadband excitation. There are five possible pairs of signals that can be used with an external summing junction, and there are three possible pairs that can be used with an internal summing junction. In addition to this minimum set, two extra methods are included (3 and 16) because of their popularity, they require fewer computations and are easier to understand. Hence there are a total of 18 methods listed in table 1.

These 18 methods are ranked in order of measurement quality, so that the best possible technique can be selected for the loop gain measurement, depending upon the selected summing junction location and the available signal pairs. This ranking is somewhat flexible and depends upon variables such as the frequency region of interest, location and magnitude of disturbances (noise), analyzer accuracy,

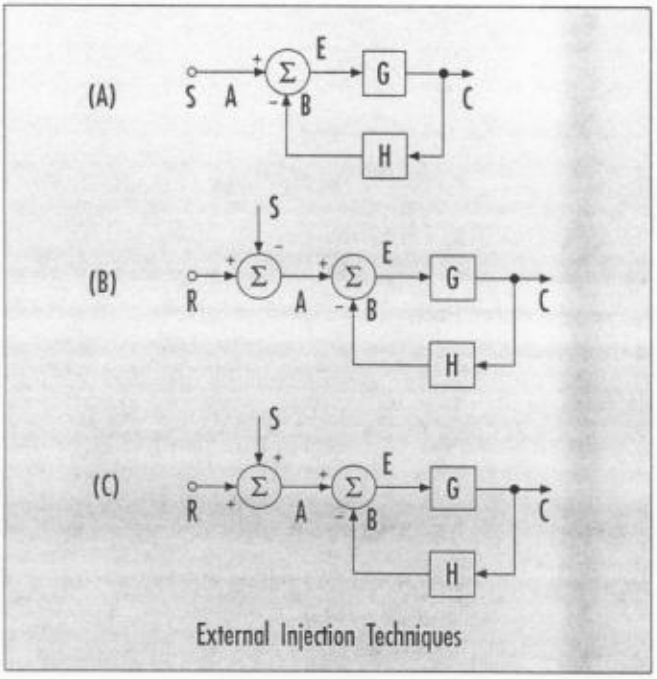

Figure 2
Injecting the excitation at a point outside the mainloop will be very convenient for many control systems.

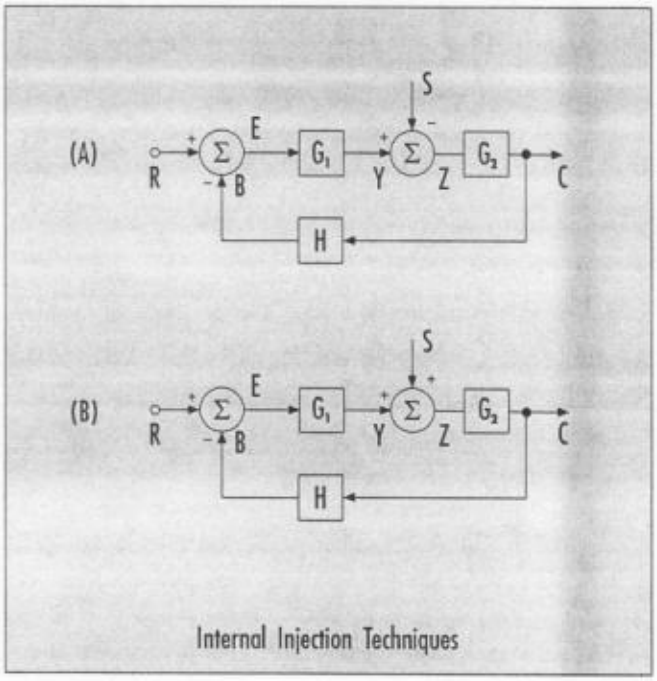

Figure 3
Some control systems do not have an accessable error summing junction. The excitation must be injected at a point inside the loop in these cases.

Basic Control Loop Testing

magnitude of the reference signal, and also the magnitude of the loop gain. Each user may need to rank these methods differently to reflect the priorities of a particular application. In any event, the ranking presented in this note should be used as a guideline, not as an inflexible rule.

Some of the many factors that can cause errors in the measurement will be summarized for each method, and calibration techniques will be described to minimize these errors. In general, methods that introduce any significant bias in the loop gain estimate are ranked low, along with methods that have unusually large values of variance.

As a general rule, any of the methods will work fine if the loop-gain magnitude is less than about 30, and if the ac[4] signal power on the reference input and on any internally generated loop-noise source is sufficiently small compared to the injected test-signal power. In two cases (methods 3 and 16), the reference-signal power and the power from other noise signals will cause a bias in the loop-gain measurement, and in several cases these signals contribute extra variance to the gain estimate. If the loop gain is very large, some methods may be heavily biased, and in some cases the variance can be excessively large.

Figure 1 shows the block diagram of a basic control system and also shows the terminology used for the various signals. This terminology is compatible with that used in reference [2], Hewlett-Packard Application Note 243-2: *Control System Development Using Dynamic Signal Analyzers.*

The loop comprises a forward gain section consisting of two elements, G_1 and G_2. The total forward gain is the product of these two which is G_1G_2. The loop also has a feedback section denoted by H, and a primary (or error) summing junction. This summing junction is where the feedback signal, B, is subtracted from the desired reference signal, R, giving the error signal E.

Figure 4 shows the Nyquist or GH-plane, where $GH=G_1G_2H$ is the loop gain of the system. It is convenient to think of GH as a complex number that varies as a function of frequency. Each control loop characteristic can be plotted as a locus of complex values on the GH-plane (called the Nyquist plot). The locus shown in figure 4 is an example of a two-pole transfer function having a dc gain of 400. The frequency increases along the locus starting at the dc point. It is important that the locus of loop gain does not encircle the point (-1,0), or the system will be unstable[5].

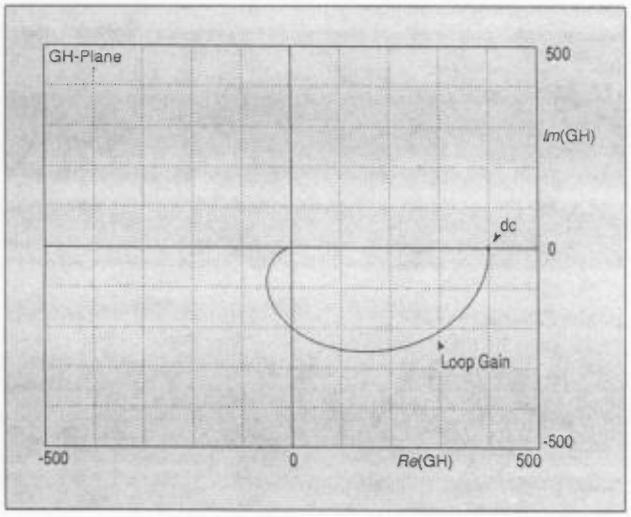

Figure 4
A typical Nyquist plot (GH-plane) of a second order control loop having a dc-loop gain of 400.

[4]Alternating current. In this note "ac" means "at all non-zero frequencies" or "at all frequencies above dc."

[5]This is a simplification of the complete "rule." For the full details, please see the discussion of the Nyquist Stability Criterion that can be found in reference [2] or in most textbooks on Classical Control Theory.

Test Signal Injection

If possible, loop measurements should be made by replacing the reference signal R with the desired excitation signal S as shown in figure 2a. The most significant advantage of this approach is that it eliminates the possibility of the reference signal affecting the measurement. Note that it is nearly as beneficial to keep the reference signal at a constant dc value.

If this is not possible, then an additional external summing junction can be inserted as shown in figure 2b or 2c. Alternately, an internal summing junction can be inserted as shown in figure 3a or 3b. In these figures the forward gain block, G, has been split into two parts G_1 and G_2, to illustrate that the summing junction can be located inside of G, if necessary. In general, the internal summing junction can be inserted anywhere within the loop. The primary concerns are the ability to match the input and output impedances of the circuit under test and the convenience of inserting the summing junction at that particular point.

It is helpful to keep the amplitudes of the various signals in mind when planning a control loop measurement. When the loop gain is high[6], the error signal E is small compared to R and B which are nearly equal in magnitude. When the loop gain is low, B is the small signal, and R and E are nearly equal. In either case, the relative error between the two measurement channels will have an exaggerated effect upon the loop gain if a pair of nearly equal signals are used. It is generally best to choose a pair of signals having dissimilar amplitudes whenever possible.

Measurement Procedure

The control system loop gain information is carried by various pairs of signals in the control loop, leading to the eighteen measurement methods that are discussed in this note. Note, however, that most of these techniques do not measure the loop gain directly. Instead, the loop gain must be calculated from the measurement.

A typical FFT-type analyzer measures the frequency response between two points in a system by forming the ratio between the cross-power spectrum between the channels, and the auto-power spectrum for channel one[7]. This measured frequency response is called T in this note. Of the 18 methods discussed in this note, 10 are of the FFT type. In eight of these the loop gain estimate, GH, is determined by performing calculations on T.

In the other two methods, GH is calculated directly from the auto-power spectrums and the cross-power spectrum that were measured. One easy-to-visualize advantage of this approach is that it is possible for these calculations to use the channel 2 auto-power spectrum, thus utilizing information that is not used when computing the frequency response, T, by means of the trispectrum average technique.

Table 1 lists the various methods discussed in this note. The indicated figure gives a graphical view of the connections. Also shown are the calculations that are required to compute GH. In some analyzers, these calculations can be performed automatically as part of the measurement procedure using the built-in waveform math feature.

[6]Roughly speaking, a system may be considered as having "high gain" when the loop gain gets greater than 20 to 30 dB (k=10 to k=30).

[7]This technique is often called the "trispectrum average" technique because of the need to average the three spectrums mentioned above. Reference [4] has more information on this subject.

Number	Method	Rank	Figure	Measure $\hat{T}=$	Calculate $\hat{GH}=$	Comments
1	B+E	1	6	$\frac{\overline{BE^*}}{\overline{\lvert E\rvert^2}}$	$\frac{\overline{B(B+E)^*}}{\overline{E(B+E)^*}}$	No bias, mininum variance
2	BSE	3	6	$\frac{\overline{BS^*}}{\overline{ES^*}}$	$\hat{T}$	No bias, low variance
3	B/E	12	6	$\frac{\overline{BE^*}}{\overline{\lvert E\rvert^2}}$	$\hat{T}$	Potential bias, minimum variance
4	ESA	4	7	$\frac{\overline{ES^*}}{\overline{AS^*}}$	$\frac{1-\hat{T}}{\hat{T}}$	Low bias, low variance
5	E/A	2	7	$\frac{\overline{EA^*}}{\overline{\lvert A\rvert^2}}$	$\frac{1-\hat{T}}{\hat{T}}$	Low bias, minimum variance
6	ESS	5	8	$\frac{\overline{ES^*}}{\overline{\lvert S\rvert^2}}$	$-\frac{1+\hat{T}}{\hat{T}}$	Low bias, low variance
7	E/S	5	8	$\frac{\overline{ES^*}}{\overline{\lvert S\rvert^2}}$	$-\frac{1+\hat{T}}{\hat{T}}$	Indentical to no. 6
8	BSA	9	9	$\frac{\overline{BS^*}}{\overline{AS^*}}$	$\frac{\hat{T}}{1-\hat{T}}$	Potential bias, high variance
9	B/A	8	9	$\frac{\overline{BA^*}}{\overline{\lvert A\rvert^2}}$	$\frac{\hat{T}}{1-\hat{T}}$	Potential bias, high variance
10	BSS	11	10	$\frac{\overline{BS^*}}{\overline{\lvert S\rvert^2}}$	$-\frac{\hat{T}}{1-\hat{T}}$	Potential bias, high variance
11	B/S	11	10	$\frac{\overline{BS^*}}{\overline{\lvert S\rvert^2}}$	$-\frac{\hat{T}}{\left(1+\hat{T}\right)}$	Identical to no. 10
12	Z/S	7	11	$\frac{\overline{ZS^*}}{\overline{\lvert S\rvert^2}}$	$-\frac{1+\hat{T}}{\hat{T}}$	low bias, medium variance
13	ZSS	7	11	$\frac{\overline{ZS^*}}{\overline{\lvert S\rvert^2}}$	$-\frac{1+\hat{T}}{\hat{T}}$	Identeical to no. 12
14	Y−Z	6	12	$\frac{\overline{YZ^*}}{\overline{\lvert Z\rvert^2}}$	$\frac{\overline{Y(Y-Z)}}{\overline{Z(Y-Z)}}$	Low bias, medium variance
15	YSZ	6	12	$\frac{\overline{YS^*}}{\overline{ZS^*}}$	$-\hat{T}$	Similar to no. 14
16	Y/Z	13	12	$\frac{\overline{YZ^*}}{\overline{\lvert Z\rvert^2}}$	$-\hat{T}$	Potential bias, medium variance
17	YSS	10	13	$\frac{\overline{YS^*}}{\overline{\lvert S\rvert^2}}$	$\frac{\hat{T}}{\left(1-\hat{T}\right)}$	Potential bias, high variance
18	Y/S	10	13	$\frac{\overline{YS^*}}{\overline{\lvert S\rvert^2}}$	$\frac{\hat{T}}{\left(1-\hat{T}\right)}$	Identical to no. 17

Table 1
Summary of Methods

Sources of Potential Error

Regardless of which measurement technique is selected (see appendix A for a discussion of broadband and swept-sine techniques), it is important to choose a conjugate spectrum that is both coherent with the test excitation signal and as incoherent as possible with the noise component of either the numerator or the denominator spectrum. Otherwise, a bias will be introduced into the spectral average when the product is formed. This is the problem with methods 3 and 16 as indicated in table 2.

Different measurement methods do not have the same potential for error. Swept sine methods, for example, use the conjugate of the source as the secondary spectrum in these products. Since the source is noise-free by definition, the swept sine methods have no bias due to the various noise sources in the control system (unless there are discrete sinusoids generated internal to the loop).

Some broadband methods also use the source spectrum in the spectral products, so there is no noise bias for these methods either. However, other broadband methods are forced to use the conjugate of either the numerator or the denominator spectra for the conjugate component. This means there is a potential bias in the resulting spectral averages and in the final frequency response calculation.

Even if bias due to noise is eliminated, there are still sources of possible bias due to mismatch between the two analyzer input channels and/or imperfections in the added summing junction. There are also bias errors associated with leakage that often occur when using a transformer as a summing element. Careful attention should be paid to these elements to minimize the errors associated with these components.

Of course, there are always random errors (as opposed to bias errors) caused by noise in the system. Some measurement methods are more sensitive to this noise than others. In all cases, this random error can be reduced either by averaging or by integrating for longer intervals of time.

In principle, many of these errors can be measured and subsequently removed in a calibration step described later in this note. Unfortunately, for the lower six methods in the decision tree (figure 5), it is not practical to perform this calibration step accurately enough to allow good measurements when the loop gain magnitude is large. Table 5 gives maximum practical values of loop gain magnitude for each method, and only those preceded by an asterisk can be used when the loop gain magnitude is large (>30).

In figures 6 through 13, the sources of errors that were assumed in this work are shown in dotted boxes. The dotted summing junctions do not represent real hardware summing junctions but rather imaginary or effective summing junctions that are used to illustrate where noise is assumed to be injected.

The 18 Methods

The various properties of interest for all of the methods are summarized in tables 1 through 5, and the associated block diagrams for each method are illustrated in figures 6 through 13. Figure 5 is a decision tree that can be used to select the best methods, given the availability of an internal or external summing junction, and various pairs of signals that can be probed.

In these tables, a caret (^) over any quantity denotes an estimate (or measure) of that quantity, and a tilde (~) denotes a calibrated version of that quantity. An overbar (–) denotes an averaging operation, and an asterisk (*) denotes a complex conjugate. The notation E[ ] denotes the expected value of a random variable (estimated or measured quantities are random variables).

Table 1 assigns an identification number and a name to each method, and lists the rank and figure designation associated with that method. In addition, the table shows the calculations that must be performed to obtain an estimate of the loop gain. Methods 3 and 16 would normally be replaced by methods 1 and 14, respectively, but are included because they are sometimes selected by users.

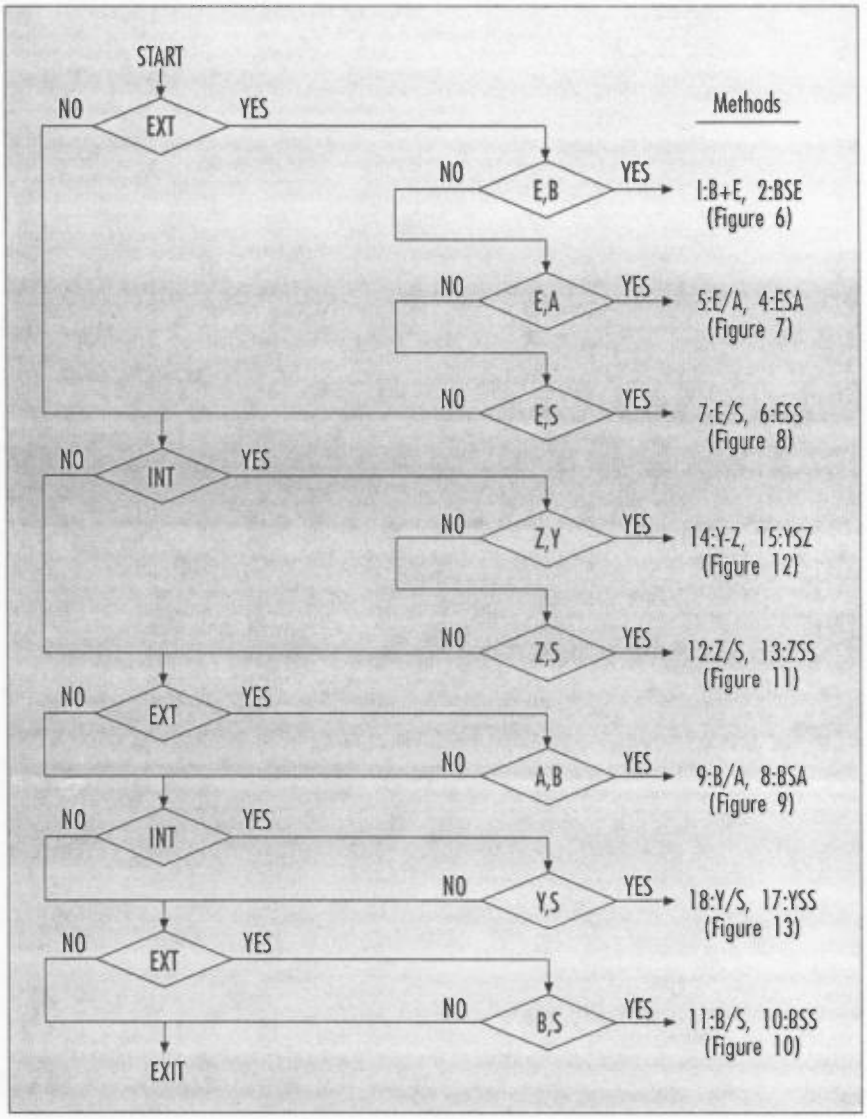

Figure 5
A decision tree for selecting the best method to use in characterizing the loop gain of a control system. The selection is based upon the choice of either an internal or an external summing junction and upon the pairs of signals in the loop that are available.

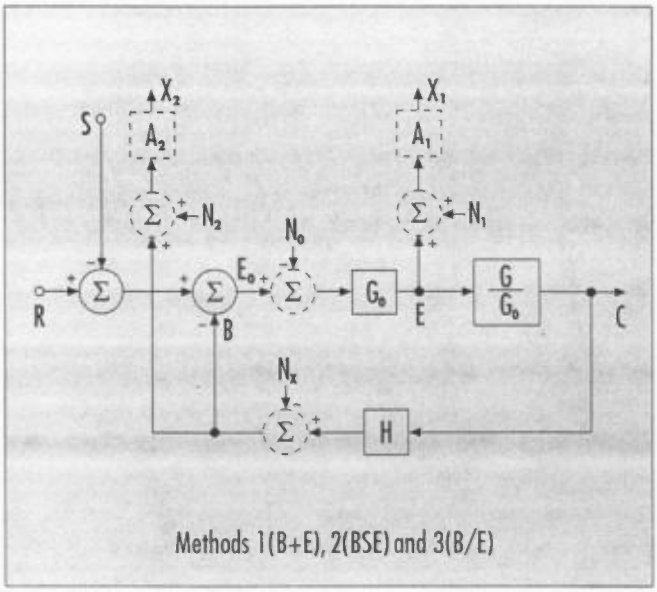

Figure 6
Block diagram of a control system, showing the added external summing junction and the analyzer connection points for the B+E, BSE, and B/E methods.

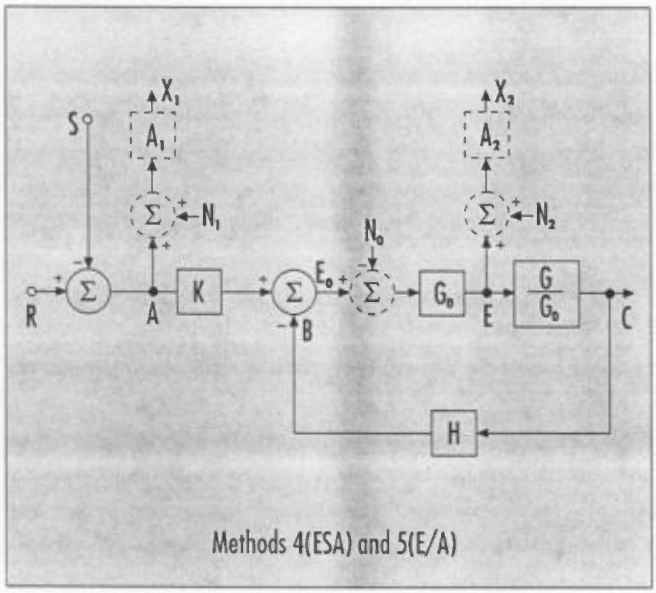

Figure 7
Block diagram of a control system, showing the added external summing junction and the analyzer connection points for the ESA and E/A methods.

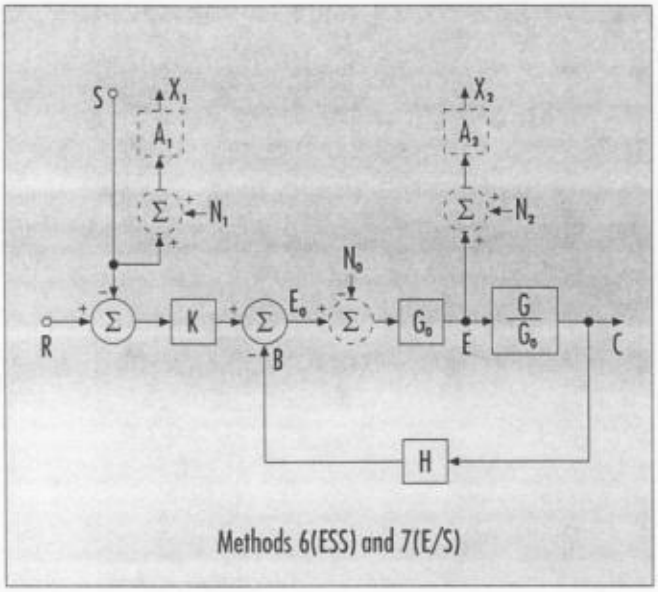

Figure 8
Block diagram of a control system, showing the added external summing junction and the analyzer connection points for the ESS and E/S methods.

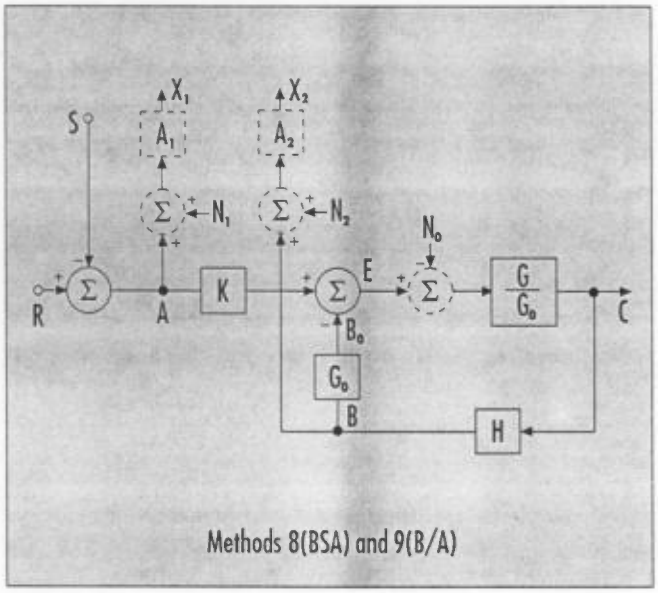

Figure 9
Block diagram of a control system, showing the added external summing junction and the analyzer connection points for the BSA and B/A methods.

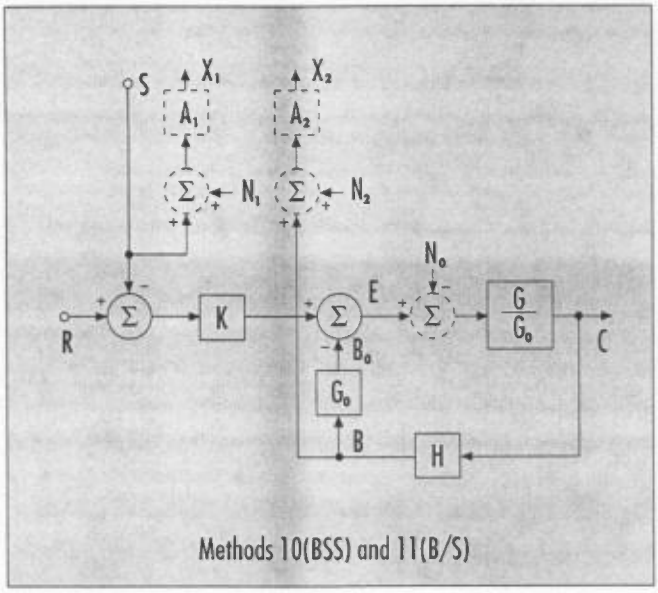

Figure 10
Block diagram of a control system, showing the added external summing junction and the analyzer connection points for the BSS and B/S methods.

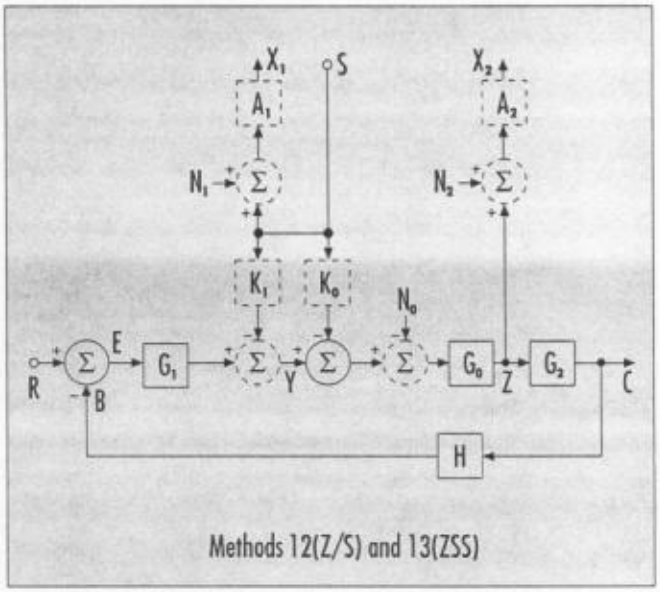

Figure 11
Block diagram of a control system, showing the added internal summing junction and the analyzer connection points for the Z/S and ZSS methods.

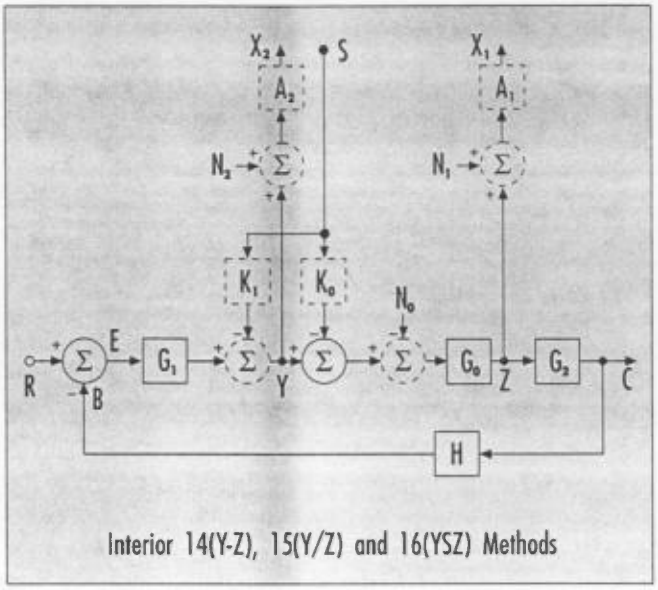

Figure 12
Block diagram of a control system, showing the added internal summing junction and the analyzer connection points for the Y-Z, Z/Y, and YSZ methods.

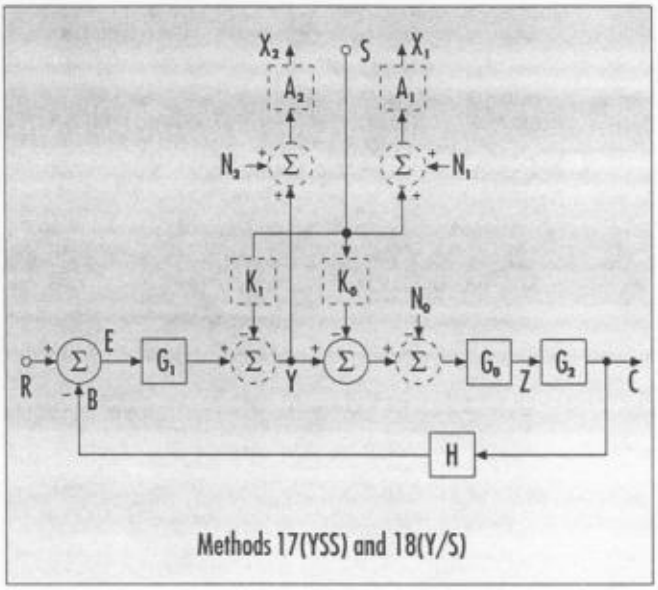

Figure 13
Block diagram of a control system, showing the added internal summing junction and the analyzer connection points for the YSS and Y/S methods.

Expected Value of Loop Gain
Table 2 lists the expected values of the loop gain estimates (as though an infinite number of averages were used in making the measurement). It is necessary to refer to the figure with the proper block diagram to understand the parameters that appear in these expected value equations. The total power in each of the various signals is denoted by sigma squared. Thus,

σ_S^2 is the total power in the excitation signal S

σ_R^2 is the total power in the reference signal R

σ_O^2 is the total power in the internal loop noise source N_0

σ_X^2 is the total power in the internal loop noise source N_X

σ_1^2 is the total noise power in channel 1 of the analyzer

σ_2^2 is the total noise power in channel 2 of the analyzer.

The internal loop noise signals N_0 and N_X represent any disturbances that might come from outside the loop, as well as any noise sources that are intrinsic to components within the loop. Noise contributions from other places in the loop can be referenced to either N_0 or N_X by the application of a suitable frequency response transformation to the actual noise spectrum.

Keep in mind that GH is the ideal result for each of these estimates. Each expression is a mapping of the expected value of the actual measurement onto

Number	Expected Value $E[\hat{GH}]=$
1	$\frac{A_2 GH}{A_1 G_0}$
2	$\frac{A_2 GH}{A_1 G_0}$
3	$\frac{A_2}{A_1 G_0}\frac{GH\left(\sigma_S^2+\sigma_R^2+\sigma_0^2\right)-\sigma_X^2}{\sigma_S^2+\sigma_R^2+\sigma_0^2+\sigma_X^2+\frac{\lvert 1+GH\rvert^2}{\lvert G_0\rvert^2}\sigma_1^2}$
4,5,6,7	$\frac{A_1}{A_2 G_0 K}\left(GH-\frac{A_2 G_0 K}{A_1}+1\right)$
8,9,10,11	$\frac{A_2 K_0}{A_1 G_0}\frac{GH}{1+GH\left(1-\frac{A_2 K}{A_1 G_0}\right)}$
12,13	$\frac{A_1}{A_2(K_0+K_1)}\left(GH-\frac{A_2(K_0+K_1)}{A_1}+\frac{1}{G_0}\right)$
14,15	$\frac{A_2 K_0}{A_1(K_0+K_1)}\left(GH-\frac{K_1}{K_0 G_0}\right)$
16	$\frac{A_2}{A_1 G_0}\frac{(K_0+K_1)^*(K_0 G_0 GH-K_1)\sigma_S^2-\lvert G_1\rvert^2\sigma_R^2+G_0 GH\sigma_0^2}{\lvert K_0+K_1\rvert^2\sigma_S^2+\lvert G_1\rvert^2\sigma_R^2+\left\lvert GH+\frac{1}{G_0}\right\rvert^2\sigma_1^2}$
17,18	$\frac{A_2 K_0 G_0}{A_1+A_2 K_1}\frac{GH-\frac{K_1}{K_0 G_0}}{1+\frac{A_1-A_2 K_0}{A_1+A_2 K_1}G_0 GH}$

Table 2
Summary of expected values of loop gain

the ideal GH-plane. If there were no errors, this would be an identity mapping. The simplest type of error is a scaling error, as indicated for method 2, in which case the mapping is simply an expansion or contraction of the GH-plane around a common origin. Methods 4, 5, 6, and 7 also include an offset or bias in the estimate, so in addition to an expansion or contraction, this mapping also involves a translation of the origin.

Methods 8, 9, 10, and 11 involve a bilinear transformation, in which GH appears in a linear manner in both numerator and denominator. This is a mapping in which straight lines in the GH-plane are transformed into circles in the estimated or E[GH] plane. Figure 14 shows an example of this effect. Here a measurement error of 0.998 is assumed[8] and the resulting plot is compared against the true, or ideal plot. Note that since the ideal plot is the same 2nd-order control loop that was introduced in figure 4, it is apparent that the magnitude of GH increases as the frequency approaches dc. Thus the fact that these two plots diverge as the frequency approachs dc can also be interpreted as "the larger the loop gain, the larger the measurement error."

Figure 15 shows the same Nyquist plots with the mapping coordinates superimposed, indicating in a graphical way the cause of the error due to this channel mismatch. For example, the original point (500, 500) on the GH-plane maps into the point (300,100) on the E[GH] plane, and the original point (500,0) maps into the point (250,0).

Figure 16 shows the same mapping on an expanded scale, with a true dc-loop gain of 80 and an estimated dc-loop gain of approximately 70. The errors become smaller as the loop gain approaches unity, but even for a dc-loop gain of 30, the error is approximately -5.7%. In practice, the channel match will be a complex number as a function of frequency, so the actual mapping will be somewhat more complex than indicated here, and may include a rotation of the basic keystone pattern.

The expression for method 16 in table 2 stands out as being particularly complicated, although this is one of the most straightforward methods in the list. The expected value for this method is biased by reference signal power, internal loop noise power, and the noise power in channel 1 of the analyzer. For small to medium values of loop gain, the bias is mostly due to the reference signal. When the reference signal power becomes significant compared to the excitation signal power, there is a bias in the expected value of the loop gain for all values of gain. Thus, this method is not recommended in this situation. Method 3 has somewhat similar behavior, as indicated by the expected value expression in table 2.

[8]If all of this error was caused by the analyzer making the measurement, this represents a channel-to-channel mismatch of 0.2%.

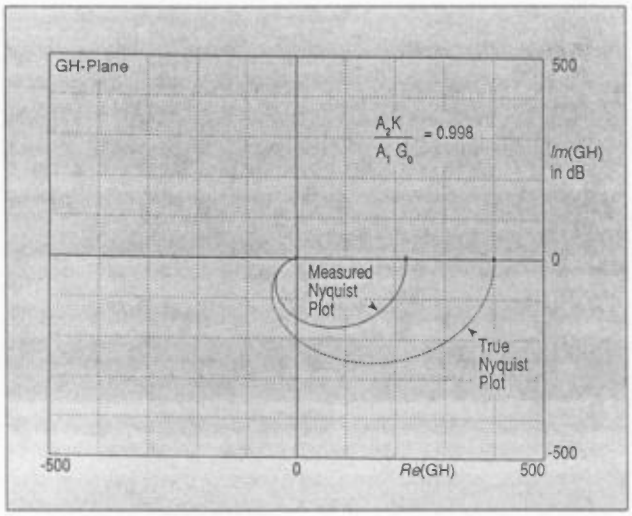

Figure 14
The GH-plane, showing the correct Nyquist plot as a dashed line and the measured plot as a solid line, using one of the methods 8, 9, 10, 11, in which the analyzer channel match is less that unity (0.998).

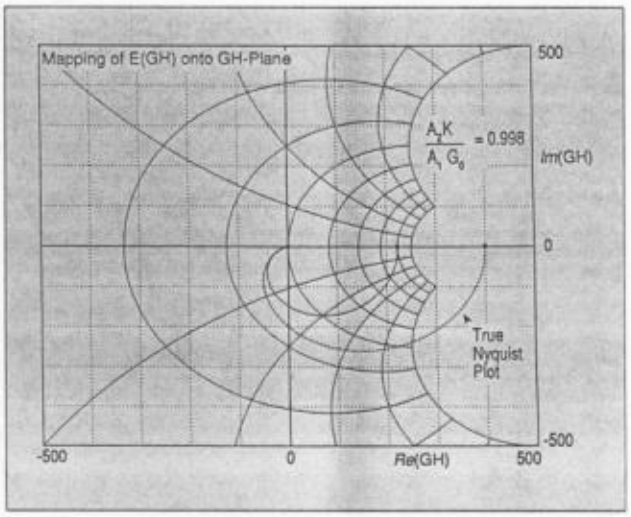

Figure 15
The solid coordinate lines represent the mapping of the expected value of GH onto the GH-plane, using one of the methods 8, 9, 10, 11, in which the analyzer channel match is set to 0.998. The GH-plane rectangular grid lines are transformed into orthogonal circles by this mapping, with the point (500,500) mapping into the point (300,100).

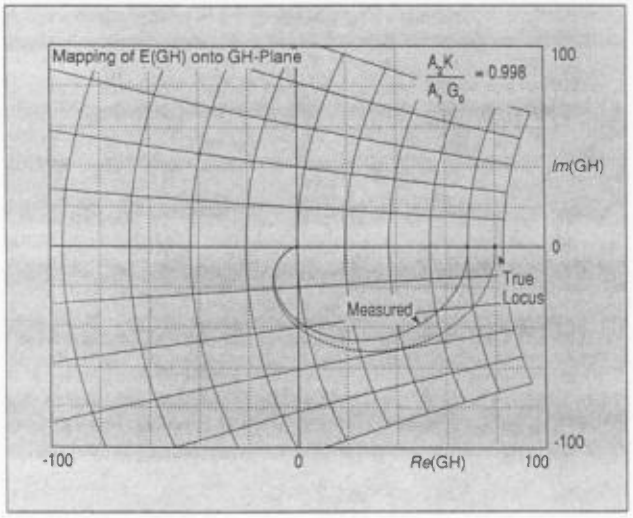

Figure 16
This is a mapping of the expected value of GH onto the GH-plane as in figure 13, except the scale is expanded to show the region around the origin. The true loop gain is 80, and the analyzer channel match remains at 0.998.

Noise-to-Signal Ratio of Loop Gain Estimate

Table 3 lists the ratio between the standard deviation and the expected value of the estimated loop gain for all of the methods of interest. This is called a noise-to-signal ratio, even though the "signal" is actually the expected value of GH. Some of these expressions are more complicated than others, but they all have a very similar form. They all have a zero near GH = -1, and they become infinite somewhere near GH = 0. They all grow in a linear manner with respect to GH, for large values of GH, and they are all reduced by the square root of the number of averages used in estimating GH.

Number	Noise-to-Signal Ratios $\eta =$
1	$\frac{\lvert 1+GH\rvert}{\lvert GH\rvert}\frac{\left(\sigma_X^2+\sigma_2^2+\left\lvert\frac{GH}{G_0}\right\rvert^2\sigma_1^2\right)^{\frac{1}{2}}}{\sqrt{n}\left(\sigma_S^2+\sigma_R^2+\sigma_0^2\right)^{\frac{1}{2}}}$
2	$\frac{\lvert 1+GH\rvert}{\lvert GH\rvert}\frac{\left(\sigma_X^2+\sigma_2^2+\left\lvert\frac{GH}{G_0}\right\rvert^2\sigma_1^2\right)^{\frac{1}{2}}}{\sqrt{n}\sigma_S}$
4 $W_0=\frac{A_2G_0K}{A_1}-1$	$\frac{\lvert 1+GH\rvert}{\lvert GH-W_0\rvert}\frac{\left(\sigma_0^2+\lvert K\rvert^2\sigma_1^2+\left\lvert\frac{1+GH}{G_0}\right\rvert^2\sigma_2^2\right)^{\frac{1}{2}}}{\sqrt{n}\lvert K\rvert\sigma_S}$
5 $W_0=\frac{A_2G_0K}{A_1}-1$	$\frac{\lvert 1+GH\rvert}{\lvert GH-W_0\rvert}\frac{\left(\sigma_0^2+\lvert K\rvert^2\sigma_1^2+\left\lvert\frac{1+GH}{G_0}\right\rvert^2\sigma_2^2\right)^{\frac{1}{2}}}{\sqrt{n}\lvert K\rvert\left(\sigma_S^2+\sigma_R^2\right)^{\frac{1}{2}}}$
6,7 $W_0=\frac{A_2G_0K}{A_1}-1$	$\frac{\lvert 1+GH\rvert}{\lvert GH-W_0\rvert}\frac{\left(\sigma_0^2+\lvert K\rvert^2\left(\sigma_R^2+\sigma_1^2\right)+\left\lvert\frac{1+GH}{G_0}\right\rvert^2\sigma_2^2\right)^{\frac{1}{2}}}{\sqrt{n}\lvert K\rvert\sigma_S}$
8 $A=1-\frac{A_1K}{A_1G_0}$	$\frac{\lvert 1+GH\rvert}{\lvert GH\rvert\lvert 1+AGH\rvert}\frac{\left(\lvert GH\rvert^2\sigma_0^2+\lvert KGH\rvert^2\sigma_1^2+\lvert G_0(1+GH)\rvert^2\sigma_2^2\right)^{\frac{1}{2}}}{\sqrt{n}\lvert K\rvert\sigma_S}$
9 $A=1-\frac{A_1K}{A_1G_0}$	$\frac{\lvert 1+GH\rvert}{\lvert GH\rvert\lvert 1+AGH\rvert}\frac{\left(\lvert GH\rvert^2\sigma_0^2+\lvert KGH\rvert^2\sigma_1^2+\lvert G_0(1+GH)\rvert^2\sigma_2^2\right)^{\frac{1}{2}}}{\sqrt{n}\lvert K\rvert\left(\sigma_S^2+\sigma_R^2\right)^{\frac{1}{2}}}$
10,11 $A=1-\frac{A_1K}{A_1G_0}$	$\frac{\lvert 1+GH\rvert}{\lvert GH\rvert\lvert 1+AGH\rvert}\frac{\left(\lvert GH\rvert^2\sigma_0^2+\lvert KGH\rvert^2\left(\sigma_R^2+\sigma_1^2\right)+\lvert G_0(1+GH)\rvert^2\sigma_2^2\right)^{\frac{1}{2}}}{\sqrt{n}\lvert K\rvert\sigma_S}$
12,13 $W_0=\frac{A_2(K_0+K_1)}{A_1}$	$\frac{\lvert 1+G_0GH\rvert}{\lvert GH-W_0\rvert}\frac{\left(\lvert G_1\rvert^2\sigma_R^2+\sigma_0^2+\lvert K_0+K_1\rvert^2\sigma_1^2+\left\lvert GH+\frac{1}{G_0}\right\rvert^2\sigma_2^2\right)^{\frac{1}{2}}}{\sqrt{n}\lvert G_0\rvert\lvert K_0+K_1\rvert\sigma_S}$
14,15 $W_0=\frac{K_1}{K_0G_0}$	$\frac{\lvert 1+GH\rvert}{\lvert GH-W_0\rvert}\frac{\left(\lvert G_1\rvert^2\sigma_R^2+\left\lvert\frac{K_1}{K_2}\right\rvert^2\sigma_0^2+\left\lvert 1+\frac{K_1}{K_0}\right\rvert^2\sigma_2^2+\lvert GH-W_0\rvert^2\sigma_1^2\right)^{\frac{1}{2}}}{\sqrt{N}\lvert G_0\rvert\lvert K_0+K_1\rvert\sigma_S}$
17,18 $A=\frac{A_1-A_2K_0}{A_1+A_2K_1}$	$\frac{\lvert 1+G_0GH\rvert\left(\lvert G_1\rvert^2\sigma_R^2+\lvert G_0GH\rvert^2\sigma_0^2+\lvert 1+G_0GH\rvert^2\sigma_2^2+\lvert K_0G_0GH-K_1\rvert^2\sigma_1^2\right)^{\frac{1}{2}}}{\sqrt{n}\lvert K_0G_0GH-K_1\rvert\lvert 1+AG_0GH\rvert\left\lvert 1+\frac{A_2K_1}{A_1}\right\rvert\sigma_S}$

Table 3
Noise to signal ratios.

There are differences in the scale factors, determined by the various signal power quantities, and in the corner frequency where the turn-up begins, so some methods are better than others. However, figures 17 and 18 can be used to study the general behavior of the noise-to-signal ratio of all the methods. Figure 17 shows the GH-plane with a dotted coordinate system, and the noise-to-signal ratio surface is plotted above this plane. A typical Nyquist plot is shown on both the base GH-plane and on the noise-to-signal ratio surface.

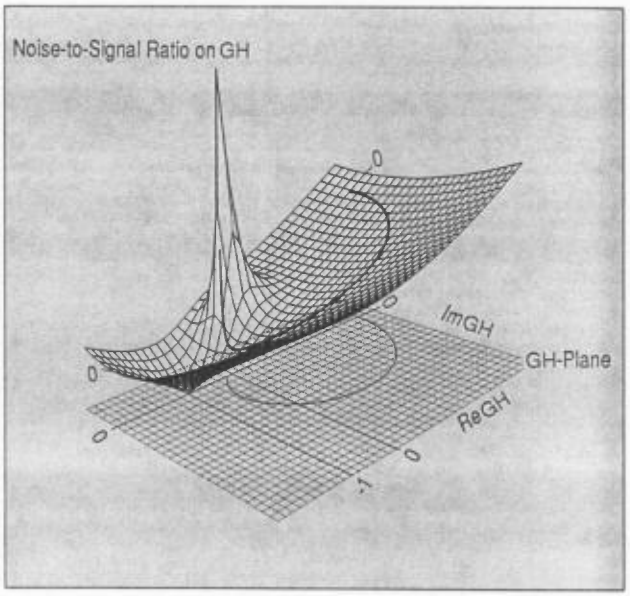

Figure 17
This is a plot of the noise-to-signal ratio on the measurement of GH, along with the base coordinates in the GH-plane as dotted lines, showing a typical Nyquist plot on both surfaces. Note the null at the point of instability (-1,0).

As indicated in figure 17, the noise-to-signal ratio tends to be best near the gain-crossover point and near the region where the gain and phase margins are measured. Thus, the most accurate measurements of the loop gain occur in this unity gain region. The various methods differ considerably in the actual values of the noise-to-signal ratio for any given value of loop gain. Expressions for this quantity are given in table 3 for each method.

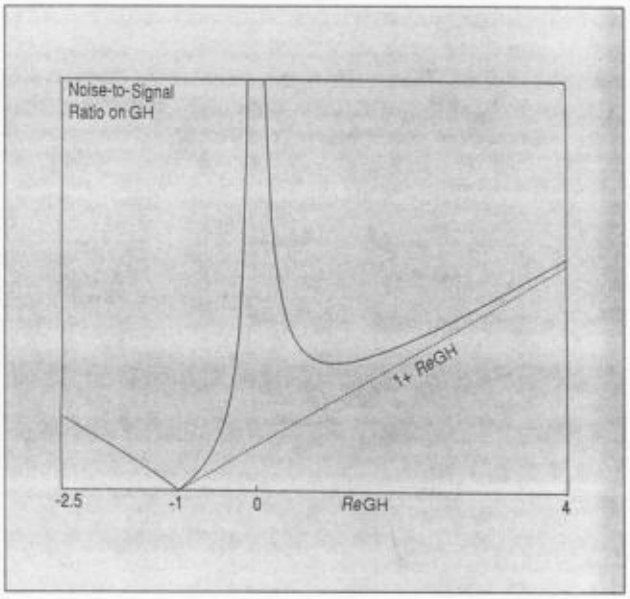

Figure 18
This is a cross-section along the real GH axis of the noise-to-signal ratio displayed in figure 18, showing the asymptotic behavior for large values of GH.

Figure 18 shows a cut along the real GH axis of this same noise-to-signal ratio plot. The zero at the point (-1,0) is apparent, as is the discontinuity at the origin. Note the linear growth with GH, as GH becomes large.

Methods 3 and 16 are omitted from table 3 because both methods may be replaced by better methods (methods 1 and 14 respectively). Also the results for both methods are rather complicated. See reference [3] for these expressions.

Calibration

Table 4 lists the calibration conditions needed to remove the various error contributions from the measurement by means of a calibration[9] procedure. To use these, the variables listed in column 2 under Calibration Conditions must be measured. After measuring these parameters one or more of the parameters must be adjusted until the expression listed in table 4 is true. The actual measurement of T can now be performed.

Alternatively, calibration "constants" can be defined and applied to the measurement results (the power spectrums, cross spectrums, and linear spectrums. Remember, though, that these "constants" will, in general, vary as a function of frequency. Also remember that no measurement is perfect. The indicated calibration conditions can, if successfully implemented, improve the accuracy of the estimate of GH. However, this should not be used as an excuse for not paying careful attention to the measurement setup. In most cases, acceptable results can be achieved without formally considering these conditions.

Whenever this calibration step is taken, the expression given for calculating $\widetilde{GH}$ should also be taken. Note that in all cases, the value of GH computed using the equations in table 1 is an approximation to the calibrated value, $\widetilde{GH}$.

Number	Calibration Conditions ($\widetilde{GH}$ is calibrated version of $\hat{GH}$)	Coherence
1	$A_2 = A_1 G_0$ $\widetilde{GH} = \hat{GH}$	$\lvert\gamma_{GH}\rvert^2 = \dfrac{\lvert\gamma_T\rvert^2\lvert 1+\hat{T}\rvert^2\lvert\gamma_T\rvert^2+\hat{T}\rvert^2}{\lvert 1+\hat{T}\rvert^2\lvert\gamma_T\rvert^2+\hat{T}\rvert^2+\lvert\hat{T}\rvert^2\left(1-\lvert\gamma_T\rvert^2\right)^3}$
2,3	$A_2 = A_1 G_0$ $\widetilde{GH} = \hat{GH}$	$\lvert\gamma_{GH}\rvert^2 = \lvert\gamma_T\rvert^2$
4,5	$A_1 = A_2 G_0 K$ $\widetilde{GH} = \hat{GH}$	$\lvert\gamma_{GH}\rvert^2 = \dfrac{\lvert\gamma_T\rvert^2\lvert 1-\hat{T}\rvert^2}{\lvert\gamma_T\rvert^2\lvert 1-\hat{T}\rvert^2+1-\lvert\gamma_T\rvert^2}$
6,7	$A_2 = A_1 G_0 K$ $\widetilde{GH} = \hat{GH}$	$\lvert\gamma_{GH}\rvert^2 = \dfrac{\lvert\gamma_T\rvert^2\lvert 1+\hat{T}\rvert^2}{\lvert\gamma_T\rvert^2\lvert 1+\hat{T}\rvert^2+1-\lvert\gamma_T\rvert^2}$
8,9	$A_1 = \dfrac{A_2 K}{G_0}$ $\widetilde{GH} = \hat{GH}$	$\lvert\gamma_{GH}\rvert^2 = \dfrac{\lvert\gamma_T\rvert^2\lvert 1-\hat{T}\rvert^2}{\lvert\gamma_T\rvert^2\lvert 1-\hat{T}\rvert^2+1-\lvert\gamma_T\rvert^2}$
10,11	$A_1 = \dfrac{A_2 K}{G_0}$ $\widetilde{GH} = \hat{GH}$	$\lvert\gamma_{GH}\rvert^2 = \dfrac{\lvert\gamma_T\rvert^2\lvert 1+\hat{T}\rvert^2}{\lvert\gamma_T\rvert^2\lvert 1+\hat{T}\rvert^2+1-\lvert\gamma_T\rvert^2}$
12,13	$A_1 = A_2(K_0 + K_1)$ $\widetilde{GH} = \hat{GH} + 1 - \dfrac{1}{G_0}$	$\lvert\gamma_{GH}\rvert^2 = \dfrac{\lvert\gamma_T\rvert^2\lvert 1+\hat{T}\rvert^2}{\lvert\gamma_T\rvert^2\lvert 1+\hat{T}\rvert^2+1-\lvert\gamma_T\rvert^2}$
14	$A_2 = A_1 G_0$ $\widetilde{GH} = \dfrac{GH(K_0+K_1)+K_1}{K_0 G_0}$	$\lvert\gamma_{GH}\rvert^2 = \dfrac{\lvert\gamma_T\rvert^2\lvert 1-\hat{T}\rvert^2\lvert\gamma_T\rvert^2-\hat{T}\rvert^2}{\lvert 1-\hat{T}\rvert^2\lvert\gamma_T\rvert^2-\hat{T}\rvert^2\lvert\hat{T}\rvert^2\left(1-\lvert\gamma_T\rvert^2\right)^3}$
15,16	$A_1 = \dfrac{A_2 K_0}{K_0 + K_1}$ $\widetilde{GH} = \hat{GH} + \dfrac{K_1}{K_0 G_0}$	$\lvert\gamma_{GH}\rvert^2 = \lvert\gamma_T\rvert^2$
17,18	$A_1 = A_2 + K_0$ $\widetilde{GH} = \dfrac{\hat{GH}(K_0+K_1)+K_1}{K_0 G_0}$	$\lvert\gamma_{GH}\rvert^2 = \dfrac{\lvert\gamma_T\rvert^2\lvert 1-\hat{T}\rvert^2}{\lvert\gamma_T\rvert^2\lvert 1-\hat{T}\rvert^2+1-\lvert\gamma_T\rvert^2}$

Table 4 Summary of Calibration Conditions and Coherence

[9]Calibration, as used here, does not refer to the normal calibration done by an instrument to ensure that the accuracy of the instrument is within the specified limits, but rather to an extra step taken to correct for known measurement errors.

Coherence, and Maximum Loop Gain

Table 4 also lists expressions for calculating the coherence function that corresponds to the loop-gain estimate, given the measured frequency response and the measured coherence function. These expressions need to be evaluated if one wishes to use the coherence function as a measure of how good the measurement is or as an input to a curve fitter.

Finally, table 5 lists expressions for the maximum loop-gain magnitude that can be handled by each method. There are two groups of measurements in this list. Those marked with an asterisk are good for large loop gain magnitudes, and the maximum magnitude is limited by the ratio of excitation signal amplitude to analyzer noise amplitude. The remaining methods are not good for large loop gain magnitudes, and are limited by the mismatch between the analyzer channels or summing junction channels.

For the first group of methods, the maximum loop gain can be increased by averaging more spectra. Unfortunately, nothing much can be done to improve the performance of the second group of measurements, other than to improve the accuracy of the measurement.

Number	$\lvert GH\rvert_{max}$	Note
*1	$\frac{\sqrt{n}}{10}\left(\frac{\sigma_S^2+\sigma_R^2+\sigma_0^2}{\sigma_1^2}\right)^{\frac{1}{2}}$	$\sigma_1 \langle \sigma_2$
*2	$\frac{\sqrt{n}}{10}\frac{\sigma_S}{\sigma 1}$	$\sigma_1 \langle \sigma_2$
3	Same as method 1 for σ_x and σ_1 small	$\sigma_1 \langle \sigma_2$
*4	$\frac{\sqrt{n}}{10}\frac{\sigma_S}{\sigma_2}$	$\sigma_2 \langle \sigma_1$
*5	$\frac{\sqrt{n}}{10}\left(\frac{\sigma_S^2+\sigma_R^2}{\sigma_2^2}\right)^{\frac{1}{2}}$	$\sigma_2 \langle \sigma_1$
*6,7	$\frac{\sqrt{n}}{10}\frac{\sigma_S}{\sigma_2}$	$\sigma_2 \langle \sigma_1$
8,9,10,11	$\frac{1}{10}\frac{\lvert A_1G_0\rvert}{\lvert A_1G_0 - A_2K\rvert}$	$\sigma_1 = \sigma_2$
*12,13	$\frac{\sqrt{n}}{10}\frac{\sigma_S}{\sigma_2}$	$\sigma_2 \langle \sigma_1$
*14,15	$\frac{\sqrt{n}}{10}\frac{\sigma_S}{\sigma_1}$	$\sigma_1 \langle \sigma_2$
16	Same as methods 14, 15 for $\sigma_S^2 \rangle\rangle \lvert G_1\rvert^2 \sigma_R^2 + \sigma_0^2$	$\sigma_1 \langle \sigma_2$
17,18	$\frac{1}{10}\frac{\lvert A_1 + A_2K_1\rvert}{\lvert A_1 - A_2K_0\rvert}$	$\sigma_1 = \sigma_2$

Table 5
Summary of Maximum Possible Loop Gain Magnitudes

Choosing Methods

No one technique is best in all cases. In fact, because of the wide variety of configurations of control systems, each of these methods might be the "correct" choice in some particular situation. Figure 5 is a decision tree that can be used to help decide on the best measurement method in any given case. One consideration is whether the reference signal can be replaced by the test signal, or will a summing junction have to be used? Is an external or an internal summing junction available? If not and one has to be added, which type will be used?

The type of excitation that will be used must also be determined. Note that for each combination of summing junction location and signal pair, there is a broadband and a swept sine excitation method that can be used and that have a similar ranking.

All of these expressions were derived based upon the assumption that all signals (S, R, N_o, N_x, N_1, N_2) are incoherent with one another and that the variances on N_1 and N_2 are small compared to the variance on S. There are numerous terms in the equations that have been discarded based upon these assumptions. In cases where these assumptions are not valid, the equations should be rederived.

Summary

A number of methods are required for measuring the loop gain of a closed loop control system, partly due to the number of different pairs of signals that might be available and partly due to the number of possible conjugate spectra that can be used to form auto- and cross-spectrum averages. There are five pairs of signals that can be used with a summing junction external to the control loop, and there are three pairs that can be used with an internal summing junction. For each pair of signals, there is a method utilizing a broadband-excitation source and a method utilizing a swept-sine source.

Thus, a total of 16 measurement methods are needed to cover all possible situations. In addition, there are two "direct" methods (3 and 16) that do not require any subsequent computations and are included because they seem to be popular. Unfortunately, they have potential bias problems and are not recommended for use in certain cases. This adds up to a total of 18 measurement methods that are discussed.

Figure 5 shows a decision tree that helps to select the best method, depending upon the location of the summing junction and upon the signal pairs that are available. It is usually better to use an external summing junction if possible, and the best approach is to simply replace the normal reference signal, R, with the test excitation signal, S. Otherwise, an internal summing junction can be used. For large loop gain magnitudes, it is necessary to select one of the upper 10 methods in the decision tree. The maximum loop gain magnitude is limited for the lower six methods, due to the unavoidable mismatch between analyzer input channels.

The variance on the loop gain estimate is a function of the loop gain itself. The ratio of the standard deviation (square root of the variance) to the expected value of the loop gain is called the noise-to-signal ratio on the estimate of GH. This noise-to-signal ratio goes to zero near the loop instability point (-1,0) in the GH-plane. This ratio becomes infinite somewhere near the GH-plane origin, and it also becomes infinite as the magnitude of GH becomes infinite.

The several methods discussed in this application note serve as a guide to techniques for modeling and analyzing a generic control system, but are really not a substitute for a specific model and for a detailed analysis of a particular control system configuration. There are too many variations in the model and in the available measurement algorithms to cover every possibility in one application note. Each control system configuration seems to have a personality of its own and deserves individual attention.

Appendix A: Excitation Signals in Control

There are two types of excitation signals that are commonly used in control system testing: broadband and swept (or stepped) sine. In the broadband case, a random signal or a chirp having a restricted bandwidth is often used, and the input and output power spectra for the control system, along with the cross-spectrum, are averaged to reduce the variance on the measurement. In the swept-sine case, the analytic source sinusoid is used to multiply both input and output channels and the results are averaged (or integrated) for some period of time to reduce the variance.

In both cases, the averaging process can be viewed as a filtering operation that introduces an effective noise-power bandwidth inversely proportional to the averaging time.

The primary difference in the measurement algorithm between these two excitation approaches is in the choice of the conjugate spectrum used in forming the auto and cross power spectrum. If a signal spectrum is multiplied by the conjugate of itself, a bias will be introduced if there is any noise or interference in the original spectrum. This bias can be eliminated by choosing a conjugate spectrum that is heavily correlated with the excitation signal, but uncorrelated with any other components. Thus, the swept sine methods tend to be unbiased, while the broadband methods may have bias unless some precautions are taken. It is important to select the conjugate spectrum with care, to minimize this bias.

Either broadband or swept sine excitation can be used. However, a swept sine test will generally be much slower than a broadband method for the same frequency span, resolution, and number of measurement points. The extra measurement time has a major benefit: swept sine results contain little or no variance. For this reason many users prefer the swept sine approach. However, if the measurement times are adjusted to be the same (for example, by increasing the number of averages in the broadband case) and if the number of measurement points is identical, the variance should be nearly the same.

In an attempt to increase the speed of the swept sine measurement, the settings for the "settling time" or the "integration time" are often reduced. Reducing these parameters too far can deteriorate the quality of the measurement by causing excessive smearing or leakage. The sweep speed should be slow enough that this does not occur.

When auto-ranging is used, a swept sine measurement can be made over a much greater dynamic range than can a broadband measurement, since the effective dynamic range is the combination of the intrinsic dynamic range of the amplifier (and analog-to-digital converter), and the dynamic range of the input attenuator. For broadband excitation, the input attenuators must be set for the total signal amplitude, so auto-ranging during the measurement is not an option.

Both methods may take extra time if there is some inefficiency in implementation. For example, time may be lost in broadband methods during the computation of the Fourier transform. For swept sine methods, time is lost in waiting for the system under test to settle after a new frequency is selected. This lost time can be quite long if the system under test contains a conjugate pair of poles near the jw-axis (i.e. lightly damped).

Appendix B: A Word on Summing Junctions

There are many ways to sum an excitation signal into the control loop, and each method should be modeled and analyzed to determine the errors that might be introduced into the measurement by the summing junction. However, the two most common injection methods use either operational amplifiers or transformers.

Using Operational Amplifiers

Figures B-1 and B-2 show two operational amplifier configurations that are commonly used. Errors are introduced into the measurement by a gain mismatch between the two input channels, both at dc and as a function of frequency. In addition, there may be an overall gain error versus frequency after the signals have been summed together. The parameters designated G_0 and K (or K_0) are used in the measurement models to account for these gain errors.

Care must be taken to properly account for the polarities of the input and output signals when the summing junction is inserted into the control loop. The polarity of the existing control system path must not be accidentally inverted when the summing junction is installed. Also, the measurement models assume a negative polarity on the excitation signal input, so this polarity must be correct, or else the model equations must be modified accordingly.

Care must also be taken to ensure that the input and output impedances of the summing junction closely match the load and drive impedances at the insertion point. If there is a significant mismatch then the resulting injection loss will cause the loop to operate differently than it will once the summing junction is removed. In general, the best place to insert an op-amp type summing junction is at a point where the input impedance is high and the drive impedance is low.

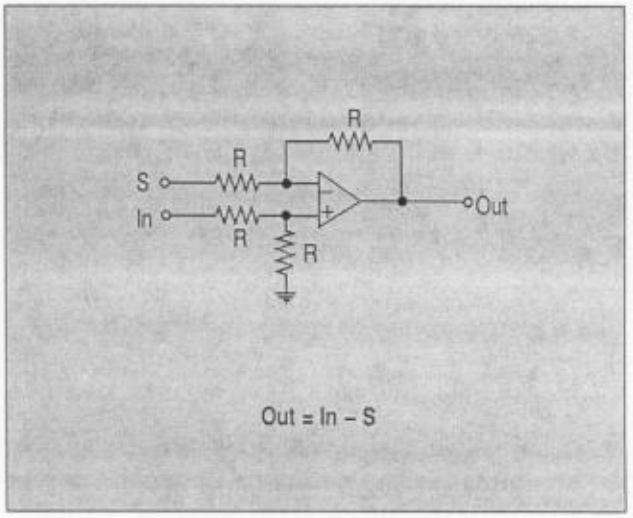

Figure B-1
A simple summing junction using an operational amplifier and four identical resistors.

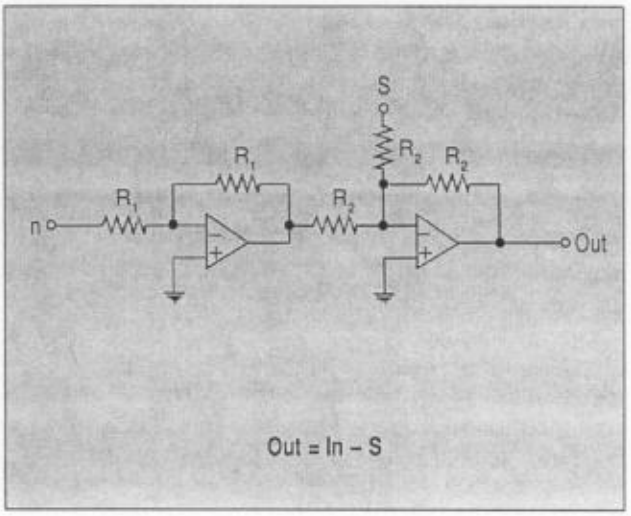

Figure B-2
An alternate summing junction topology using two operational amplifiers and five resistors, with all terminals operating at either ground or virtual ground.

Using a Transformer

In some cases, a transformer is a more convenient summing device than an operational amplifier. This is particularly true when the summing junction is located at a high voltage point in the system, or where operating currents are large (as in a switching power supply, for example). The frequency response of a transformer is generally restricted in bandwidth somewhat more than that of an operational amplifier, and transformers also tend to pick up interfering signals from various stray magnetic fields, unless adequately shielded.

When a transformer is used as an internal summing junction, there will be some degree of leakage of the input excitation signal around the transformer that can cause significant errors in the measurement. Figure B-3 shows the equivalent circuit of a summing transformer, and figure B-4 shows the equivalent model that is used for the transformer in the various measurement methods. The leakage contribution represented by K_1 is proportional to the product $Z_0(Y_L+rY_i)$. See reference [3] for a derivation of the elements of the model from the transformer equivalent circuit.

To minimize the signal leakage contribution, select a transformer with an electrostatic (Faraday) shield between the primary and secondary windings. Also keep in mind that the transfer function through a transformer may depend upon the amount of dc current that flows through a winding, due to core saturation. These dc currents will also cause larger amounts of nonlinear distortion. Be sure to select a transformer with enough magnetizing inductance to support the lowest test frequency of interest in the given impedance environment.

This leakage around the summing point is not of great concern when the transformer is used as an external summing junction, since the effects of this leakage can be accommodated by adjusting the amplitudes of the excitation S and the reference R, and by adjusting the gain/phase block K.

For critical measurements, it may be necessary to determine the characteristics of the transformer and to remove the associated errors from the loop gain estimate by means of a calibration procedure. Refer to table 4 for these calibration factors.

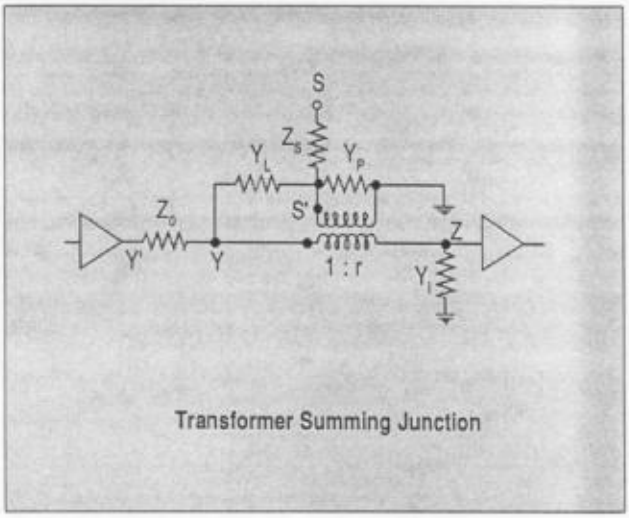

Figure B-3
The equivalent circuit of a transformer summing junction, showing a leakage path via the admittance Y_L. There is also an effective leakage term due to the product Z_0Y_i.

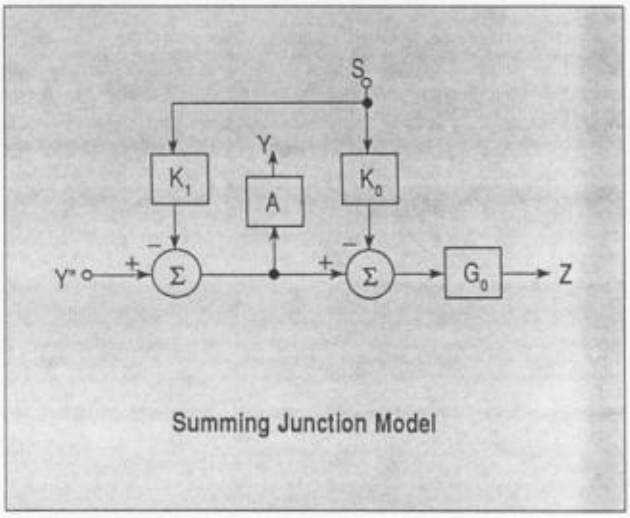

Figure B-4
A summing junction model of the transformer shown in the previous figure, in which the direct path is represented by a frequency response characteristic K_0, and the leakage path is represented by K_1 via a second summing junction.

Appendix C: Using Methods 1 and 14

A new technique, used in methods 1 and 14, of generating the conjugate spectrum by adding or subtracting the measured signals is presented in this note. Some thought must be given to the implementation of these methods since the details of how to do this may not be immediately obvious. The equations of table 1 imply that in both of these cases the loop gain can be calculated from the data generated by the trispectrum-averaging technique. Figure C-1 shows how to implement method 14, the Y-Z technique. Recall that for this measurement, the excitation signal is being injected into the loop via an internal summing junction. Channel 2 of the analyzer is connected to the input of the summing junction, Y, and channel 1 of the analyzer is connected to the output of the summing junction, Z.

$$GH = -\frac{\overline{Y(Y - Z)^*}}{\overline{Z(Y - Z)^*}}$$

$$= -\frac{\overline{Y(Y^* - Z^*)}}{\overline{Z(Y^* - Z^*)}}$$

$$= -\frac{\overline{YY^* - YZ^*}}{\overline{ZY^* - ZZ^*}}$$

$$= -\frac{\overline{YY^*} - \overline{YZ^*}}{\overline{ZY^*} - \overline{ZZ^*}}$$

$$= -\frac{\overline{YY^*} - \overline{YZ^*}}{\overline{(YZ^*)^*} - \overline{ZZ^*}}$$

$$= \frac{\overline{YZ^*} - \overline{YY^*}}{\overline{YZ^*}^* - \overline{ZZ^*}}$$

$$= \frac{\text{Cross\_Spectrum} - \text{Power\_Spectrum\_2}}{\text{Cross\_Spectrum}^* - \text{Power\_Spectrum\_1}}$$

Figure C-1 Implementing method 14 (Y-Z) using the three spectra of a trispectrum average.

The final result for method 1, B+E, is shown in figure C-2. The steps leading up to this result are similar to the steps in figure C-1.

$$GH = \frac{\overline{B(B + Z)^*}}{\overline{Z(B + Z)^*}}$$

$$= \frac{\text{Cross\_Spectrum} + \text{Power\_Spectrum\_2}}{\text{Cross\_Spectrum}^* + \text{Power\_Spectrum\_1}}$$

Figure C-2 Implementing method 1 (B+E).

Glossary

Bias. The difference between the true mean (average) value of a random variable and the expected value of some estimate of that mean.

Coherence function. The proportion of the output power from a system that is apparently caused by the input, as a function of frequency.

Conjugate spectrum. The complex conjugate of a frequency spectrum used as a common multiplier to form a numerator and denominator of a frequency response function.

Expected value. There is a precise mathematical definition, but for most purposes this is the value of a random variable after an infinite number of samples are averaged together.

Instability point. In a control system, this is the point where the loop gain magnitude is unity and the phase is -180 degrees. When this combination occurs, the loop becomes unstable.

Noise-to-signal ratio. In this note, this is the ratio of the standard deviation to the expected value of the estimate of the loop gain.

Nyquist plot. A plot of the locus of loop gain for a control system on the GH or Nyquist plane, where GH is the complex loop gain value.

Standard deviation. The square root of the variance of a random variable. This is the root-mean-square (rms) value of the random quantity.

Variance. There is a precise mathematical definition, but for most purposes the variance of a random quantity is the ac power.

References

[1]*Measuring Nonlinear Distortion Using the HP 3562A Dynamic Signal Analyzer.* Hewlett-Packard Product Note 3562A-4.

[2]*Control Systems Development Using Dynamic Signal Analyzers*, Hewlett-Packard Application Note 243-2.

[3]*Control System Measurement Techniques* and *Coherence Calculations.* Hewlett-Packard Technical Notes. Publication Numbers 5959-5760 and 5959-5761. Printed as a single document.

[4]*The Fundamentals of Signal Analysis.* Hewlett-Packard Application Note 243.